The polarity protein Yurt associates with the plasma membrane via basic and hydrophobic motifs embedded in its FERM domain

Running title: Yurt binds the plasma membrane

Clémence L. Gamblin[1,2], Charles Alende[1,2], François Corriveau[1,2], Alexandra Jetté[1,2], Frédérique Parent-Prévost[1,2], Cornélia Biehler[1,2,4,5], Nathalie Majeau[1,2], Mélanie Laurin[1,2,3], and Patrick Laprise[1,2,3,*]

[1]Centre de Recherche sur le Cancer, Université Laval, and [2]axe Oncologie du Centre de Recherche du Centre Hospitalier Universitaire de Québec-UL, 9 McMahon, Québec, QC, G1R 3S3, Canada. [3]Département de biologie moléculaire, de biochimie médicale et de pathologie, Faculté de médecine, Université Laval. [4,5]Current affiliations: Faculty of Biological and Environmental Sciences, University of Helsinki, Helsinki 00790, Finland[4]; Institute of Biotechnology, University of Helsinki, Helsinki 00790, Finland[5].

[*]Author for correspondence: Patrick.Laprise@fmed.ulaval.ca, Phone : (418) 525-4444 ext. 16959, Fax : (418) 691-5439

Key words: Yurt, membrane localization, FERM domain, FERM-adjacent domain, BH motif, epithelial cell polarity.

Summary statement

This study reveals how Yurt associates with membrane lipids in epithelial cells, thereby further illuminating the mechanisms sustaining cell polarization and tissue morphogenesis.

Abstract

The subcellular distribution of the polarity protein Yrt is subjected to a spatio-temporal regulation in *D. melanogaster* embryonic epithelia. After cellularization, Yrt binds to the lateral membrane of ectodermal cells and maintains this localization throughout embryogenesis. During terminal differentiation of the epidermis, Yrt accumulates to septate junctions and is also recruited to the apical domain. While the mechanisms through which Yrt associates with septate junctions and the apical domain have been deciphered, how Yrt binds to the lateral membrane remains as an outstanding puzzle. Here, we show that the FERM domain of Yrt is necessary and sufficient for membrane localization. Our data also establish that the FERM domain of Yrt directly binds negatively charged phospholipids. Moreover, we demonstrate that positively charged amino acid motifs embedded within the FERM domain mediates Yrt membrane association. Finally, we provide evidence suggesting that Yrt membrane association is functionally important. Overall, our study highlights the molecular basis of how Yrt associates with the lateral membrane during the developmental time window where it is required for segregation of lateral and apical domains.

Introduction

The plasma membrane of epithelial cells is segregated into an apical, a lateral, and a basal domain (Buckley and St Johnston, 2022). This structural organization, which is referred to as epithelial cell polarity, supports many unidirectional functions of epithelia. Epithelial sheets display a selective permeability owing to occluding junctions sealing the intercellular space. In *D. melanogaster*, this function is fulfilled by septate junctions, which are established laterally (Banerjee et al., 2006).

The protein Yurt (Yrt) plays a crucial role in segregating apical and lateral domains in *D. melanogaster* embryonic epithelia (Laprise et al., 2006; Laprise et al., 2009). In addition, Yrt controls septate junction permeability (Laprise et al., 2009). Yrt encloses a Four-point-one, Ezrin, Radixin, Moesin (FERM) domain at its N-terminus (Hoover and Bryant, 2002; Tepass, 2009). Yrt also contains a FERM-adjacent (FA) domain that is present in a subset of FERM family members (Baines, 2006; Tepass, 2009). The FERM and FA domain of Yrt both contribute to its oligomerization and function (Gamblin et al., 2014; Gamblin et al., 2018). The FA domain of Yrt is followed by a region lacking known protein domains designated as the variable region (VR), which ends with a putative PSD-95, DLG1, ZO-1 (PDZ) domain binding motif (PBM) (Laprise et al., 2006).

After cellularization, Yrt primarily localizes to the lateral membrane (Laprise et al., 2006). During terminal differentiation of epithelial tissues, Yrt accumulates at forming septate junctions and is recruited apically (Laprise et al., 2006; Laprise et al., 2009). While the adhesion protein Neuroglian (Nrg) recruits Yrt at septate junctions (Bieber et al., 1989; Laprise et al., 2009), the apical localization of Yrt depends on its direct interaction with Crumbs (Crb) (Laprise et al., 2006). We

74 thus gained insights into the molecular basis of Yrt association with septate junctions and the apical
75 domain, but it remains to be determined how Yrt associates with the lateral membrane basal to
76 septate junctions or prior to their formation. Furthermore, the functional importance of Yrt outside
77 of septate junctions or the apical Crb complex remains unexplored. In the present study, we
78 performed an *in vivo* structure-function analysis to define the molecular basis of Yrt association
79 with the lateral membrane in the embryonic ectoderm prior to septate junction genesis and assessed
80 the functional importance of Yrt lateral localization.
81

82 ## Results and discussion

83 **The FERM domain targets Yrt laterally *in vivo***

84 The FERM domain protein Yrt primarily associates with the lateral domain prior to septate junction
85 formation in the embryonic ectoderm of stage 10-11 *D. melanogaster* embryos [(Laprise et al.,
86 2006); Fig. 1A, B]. Similarly, immunofluorescence performed with anti-FLAG antibodies showed
87 a lateral enrichment for FLAG-tagged full length (FL) Yrt at these developmental stages ((Gamblin
88 et al., 2014); Fig. 1A, C, M), whereas FLAG-green fluorescent protein (GFP) was distributed
89 throughout cells (Fig. 1D; anti-Lethal giant larvae [Lgl] antibodies were used to visualize the lateral
90 membrane to quantify the membrane-to-cytoplasmic ratio of the GFP signal and other cytoplasmic
91 mutant proteins). This indicates that FLAG-Yrt represents a relevant model to perform a structure-
92 function analysis exploring the molecular basis of Yrt localization. We first investigated the
93 requirement of the FERM domain, the FA domain, and the VR (Hoover and Bryant, 2002; Laprise
94 et al., 2006; Tepass, 2009) for Yrt membrane localization. We found that truncated Yrt proteins
95 made of the FERM domain alone or a combination of the FERM and FA domains showed a similar
96 distribution to FLAG-Yrt FL (Fig. 1A, E, F, M), whereas removal of the FERM domain totally
97 abrogated association of Yrt with the lateral membrane (Fig. 1A, G, M). In contrast, deletion of the
98 FA domain had no significant impact on Yrt lateral distribution (Fig. 1A, H, M). Of note, FLAG-
99 Yrt$^{\Delta FA}$ and FLAG-FERM decorated the apical free surface in addition to the lateral membrane (Fig.
100 1E, H). This is consistent with our previous findings showing that phosphorylation of the FA
101 domain by atypical protein kinase C (aPKC) is required for apical exclusion of Yrt (Gamblin et al.,
102 2014). Moreover, the phosphomimetic FLAG-Yrt^{5D}, in which the aPKC phosphorylation sites in
103 the FA domain were mutated to aspartate (D) residues, showed reduced membrane-to-cytoplasmic
104 ratio (Fig. 1A, I, M; (Gamblin et al., 2014)). Finally, truncations made of the FA domain combined

105 with the VR, the VR alone, or the VR amputated from the putative PBM did not show clear
106 enrichment at the lateral domain of cells (Fig. 1A, J-M). Together, these data demonstrate that the
107 FERM domain is necessary and sufficient for Yrt membrane targeting and suggest that the FA
108 domain and the VR have a limited, if any, role in promoting Yrt lateral localization. However, the
109 FA domain likely acts as a phospho-dependent negative regulatory unit controlling Yrt association
110 with the plasma membrane.
111

112 **Yrt binds to negatively charged phospholipids and putatively directly associates with the**
113 **plasma membrane**

114 The fact that FLAG-Yrt^{5D} displays impaired membrane association led us to suggest that the
115 negative charges of the phosphomimetic residues generate electrostatic repulsion with negatively
116 charged membrane phospholipids, thereby interfering with a putative direct association of Yrt
117 FERM domain with the plasma membrane. In support of this hypothesis, the FERM domain of
118 several proteins can directly associate with phospholipids such as phosphatidylinositol 4,5-
119 bisphosphate [PI(4,5)P2] via electrostatic interactions (Ehret et al., 2023). Similarly, purified Yrt
120 FERM domain fused to GST showed affinity for phosphatidylinositol phosphates immobilized on
121 a membrane without clear discrimination between PI(3)P, PI(4)P, PI(5)P, PI(3,4)P2, PI(3,5)P2,
122 PI(4,5)P2, or PI(3,4,5)P3 (Fig. 2A). The negatively charged phosphate group(s) on
123 phosphatidylinositol phosphates is/are required for binding, as GST-FERM only faintly associated
124 with unphosphorylated Phosphatidylinositol (PI) (Fig. 2A). GST-FERM also associated with
125 Phosphatidic Acid (PA) and Phosphatidylserine (PS) (Fig. 2A). However, the FERM domain of
126 Yrt did not interact with Lysophosphatidic Acid (LPA), Lysophosphocholine (LPC),
127 Phosphatidylethanolamine (PE), Phosphatidylcholine (PC), or Sphingosine-1-phosphate (S1P)
128 (Fig. 2A). To test the specificity of our assay, we used GST alone or GST fused to the VR portion

129 of Yrt, which does not associate with the membrane (Fig. 1K), as negative controls. Strikingly,
130 these proteins did not show evident lipid binding (Fig. 2A). We also used the PI(4,5)P2 probe GST-
131 Grip that mainly associated with PI(4,5)P2 (Fig. 2A), as expected (Barnett et al., 2019), thereby
132 showing the validity of our assay. Together, these results show that the FERM domain of Yrt can
133 directly associate with selected lipids such as phosphatidylinositol phosphates but is not a
134 promiscuous lipid-binding protein. This indicates that Yrt may bind the plasma membrane by
135 interacting with charged phospholipids. To test this premise, we decreased the level of plasma
136 membrane PI(4,5)P2 in S2 cells using ionomycin, which leads to PI(4,5)P2 hydrolysis via
137 phospholipase C activation (Sparks et al., 2011). In addition, we used the PI3-kinase inhibitor
138 wortmannin and the PI4-kinase inhibitor phenylarsine oxide (PAO) to decrease the level of some
139 phosphatidylinositol phosphate species phosphorylated at position 3 and/or 4 (Dong et al., 2015;
140 Wymann et al., 2003). FLAG-Yrt was confined at the periphery in cells treated with the vehicle
141 DMSO, whereas it also localized in the cytoplasm in presence of ionomycin or wortmannin and
142 PAO (Fig. 2B-I). Residual membrane association in presence of these inhibitors is consistent with
143 the fact that Yrt can interact with most phosphatidylinositol phosphates and other lipids (Fig. 2A).
144 This also likely explains why PAO and wortmannin have a weak impact on Yrt localization when
145 used separately (Fig. 2E, F, I). Together, these data suggest that Yrt directly associates with
146 phosphatidylinositol phosphates at the lateral membrane in epithelial cells prior to septate junction
147 assembly in *D. melanogaster* embryos, a developmental time window where Yrt contributes to
148 maintaining apical-basal polarity (Laprise et al., 2009).
149

150 **Positively charged amino acids within the FERM domain target Yrt to the membrane**

151 Positively charged basic and hydrophobic (BH) amino acid motifs bind membrane phospholipids
152 via electrostatic interactions and contribute to membrane association of selected polarity proteins

153 (Bailey and Prehoda, 2015; Brzeska et al., 2010). Analysis of Yrt sequence revealed the presence
154 of two BH motifs within the FERM domain (regions of the black curve extending above the
155 threshold of 0.6 in Fig. 3A (Bailey and Prehoda, 2015)), which we referred to as BH1 and BH2.
156 Specifically, the BH1 and BH2 motifs span from amino acids 125-130 and 283-293, respectively.
157 *In silico* analysis showed that replacement of the positively charged lysine (K)124, arginine (R)132,
158 and K134 by negatively charged D residues abolished the BH properties of the BH1 motif (Fig.
159 3A, orange curve). Strikingly, FLAG-Yrt^{K124D,R132D,K134D} (FLAG-Yrt$^{BH1K/R>D}$ hereafter) displayed
160 a strongly decreased membrane-to-cytoplasmic ratio (Fig. 3B, D). Similarly, replacement of K285
161 and K288 by D residues within the BH2 motif (FLAG-Yrt$^{BH2K>D}$) decreased Yrt membrane
162 enrichment, but the effect on Yrt localization resulting from BH2 mutations was less pronounced
163 than BH1 mutations (Fig. 3C, D). Of note, the BH2K>D mutant has a BH score close to the
164 threshold of 0.6 (Fig. 3A, purple curve). This potentially explains the weak impact of the BH2K>D
165 mutations on Yrt membrane localization. To test this hypothesis, we additionally substituted the
166 last two K residues of the BH2 motif by alanine (A) residues (K292 and K293; FLAG-
167 Yrt$^{BH2K>D,K>A}$). These mutations strongly decreased the BH score (Fig. 3A, blue curve) and led to
168 a strong reduction of Yrt membrane-to-cytoplasmic ratio in S2 cells, which was more significant
169 than the delocalization of FLAG-Yrt$^{BH2K>D}$ and similar to FLAG-Yrt$^{BH1K/R>D}$ (Fig. 3E-J). Together,
170 these results demonstrate that BH1 and BH2 both contribute to target Yrt at the membrane and
171 likely do so via electrostatic interactions. Interestingly, these motifs are conserved in vertebrate
172 orthologs of Yrt (*i.e.* EPB41L4B and EPB41L5 (Tepass, 2009); Fig. S1), thereby suggesting that
173 direct membrane binding is an evolutionarily conserved property of these proteins.
174
175 **Yrt lateral localization is functionally important**

176 Yrt overexpression is associated with a gain-of-function phenotype resulting from altered aPKC
177 and Crb functions (Biehler et al., 2021; Gamblin et al., 2014). Consequently, FLAG-Yrt expression
178 causes epithelial morphogenesis defects and a fully penetrant embryonic lethality phenotype
179 (Gamblin et al., 2014; Gamblin et al., 2018). Similarly, the membrane-associated protein FLAG-
180 FERM-FA is fully lethal (Fig. 4A). FLAG-Yrt$^{BH1K/R>D}$ and FLAG-Yrt$^{BH2K>D}$, which show
181 cytoplasmic delocalization with residual membrane association (Fig. 3B-D), showed a reduced
182 ability to cause embryonic lethality (Fig. 4A). Strikingly, the cytoplasmic truncations FLAG-
183 Yrt$^{\Delta FERM}$, FA-VR, VR, and VRΔPBM did not cause any lethality (Fig. 1G, J-M; 4A), although
184 these constructs showed a similar expression level to construct causing lethality (Fig. 4B). These
185 results suggest that the gain-of-function phenotype caused by Yrt overexpression reflects its lateral
186 levels, indicating that Yrt plays an important function at this subcellular location. Alternatively,
187 our data may reflect the functional importance of the FERM domain, as all mutant or truncated
188 proteins that are phenotypically silent or that cause a weak lethality phenotype enclose an impaired
189 FERM domain. To distinguish between these two possibilities, we used FLAG-Yrt^{5D}, which
190 contains phosphomimetic mutations on aPKC target sites within the FA domain while comprising
191 an intact FERM domain (Gamblin et al., 2014). FLAG-Yrt^{5D} displayed reduced membrane levels
192 concomitant with cytoplasmic accumulation and is expressed at a similar level to wild type FLAG-
193 Yrt (Fig. 1I, 4B; (Gamblin et al., 2014)). This is in line with our previous observation that ectopic
194 localization of aPKC to the lateral domain displaces Yrt from the membrane (Biehler et al., 2021).
195 Our data thus further illuminate how Yrt function is antagonized by aPKC, which likely represses
196 Yrt association with membrane phospholipids via electrostatic repulsion (this study) while also
197 preventing Yrt oligomerization and binding to Crb (Gamblin et al., 2018). Importantly, expression
198 of FLAG-Yrt^{5D} had a modest impact on embryo survival with an 80% hatching rate (Fig. 4A). This

199 is consistent with the idea that Yrt needs to associate with the lateral membrane to be fully
200 functional. However, this result must be interpreted with caution since FLAG-Yrt^{5D} displays
201 impaired oligomerization, which also contributes to Yrt function (Gamblin et al., 2018). To identify
202 a Yrt mutant protein with impaired membrane association but showing intact oligomerization, we
203 tested whether mutation of the BH1 or BH2 motifs impacts Yrt oligomerization. We found that
204 FLAG-tagged Yrt$^{BH2K>D}$ and Yrt$^{BH2K>D,K>A}$ co-precipitated with HA-Yrt similar to wild-type
205 FLAG-Yrt (Fig. 4C). This shows that these proteins maintained their ability to oligomerize. In
206 contrast, FLAG-Yrt$^{F281A,\ W283A}$ failed to associate with HA-Yrt (Fig. 4C), as predicted by our
207 previous work (Gamblin et al., 2018). FLAG-Yrt$^{BH1K/R>D}$ also showed impaired association with
208 HA-Yrt (Fig. 4C). We also expressed a construct made of GFP fused to the transmembrane domain
209 and cytoplasmic tail of Crb with FLAG-Yrt$^{BH1KR>D}$, FLAG-Yrt$^{BH2K>D}$ or FLAG-Yrt$^{BH2K>D,K>A}$ to
210 test whether mutation of the BH motifs modifies the association with Crb, which supports some
211 Yrt functions such as apical constriction and maintenance of the apical/lateral membrane ratio
212 (Biehler et al., 2021; Laprise et al., 2006; Laprise et al., 2010). FLAG-Yrt proteins with an impaired
213 BH2 motif associated with GFP-Crb like their wild-type counterpart (Fig. 4D). In contrast, the
214 FLAG-Yrt^{L236R} showed weak binding to Crb, as expected (Gamblin et al., 2018; Ohata et al., 2011),
215 so did FLAG-Yrt$^{BH1KR>D}$ (Fig. 4D). Given that overexpression of FLAG-Yrt$^{BH2K>D}$, which show
216 reduced membrane localization while maintaining its ability to oligomerize and interact with Crb,
217 is associated with reduced lethality as compared to overexpression of wild-type FLAG-Yrt or
218 membrane-bound FLAG-FERM-FA (Fig. 4A), we conclude that association of Yrt with the lateral
219 membrane is most likely important to sustain certain of its functions.
220
221 Overall, our study shows that BH motifs within the FERM domain contribute to the localization of
222 Yrt at the lateral membrane putatively through direct association with negatively charged plasma

223 membrane phospholipids, including phosphatidylinositol phosphates. Mutations of the positively
224 charged residues contained in BH motifs attenuate the Yrt gain of function phenotype, thereby
225 arguing that Yrt association with the lateral membrane is functionally important. Yrt could thus be
226 an important interactor of phosphatidylinositol phosphates allowing these molecules to perform
227 their known role in establishing and maintaining apical-basal polarity (Gassama-Diagne et al.,
228 2006; Krahn, 2020; Martin-Belmonte et al., 2007).
229

230 ## Materials and methods

231

232 **Molecular biology, transgenic fly lines, and *in vivo* expression of transgenes**

233 The In-Fusion cloning kit (Takara Bio) was used according to manufacturer's guideline to clone
234 cDNAs into pUASTattB (kindly provided by K. Basler, University of Zurich) and pGEX-6P-2 (GE
235 Healthcare Life Sciences). Full length (FL) *yrt* refers to the beta isoform, which includes all exons
236 of the *yrt* gene (Laprise et al., 2006). The resulting plasmids allowed for expression of the following
237 3xFLAG-tagged (N-terminus) Yrt proteins: ΔFERM (a.a. 1-56/346-972); VRΔPBM (a.a. 406-
238 969), BH1KR>D (K124D, R132D, K134D); BH2K>D (K285D, K288D); BH2K>D,K>A
239 (K285D, K288D, K292A, K293A). Genome Prolab (Sherbrooke, Canada) injected plasmids in *D.*
240 *melanogaster* embryos carrying an attP docking site (Groth et al., 2004). Specifically, transgenes
241 were inserted on the third chromosome (68E1; Bloomington *Drosophila* Stock Center (BDSC) line
242 24485, which was generated by the Basler's group) or the second chromosome (25C6; line
243 produced by Genome Prolab). The other constructs and fly lines used in this study were previously
244 described (Gamblin et al., 2014; Gamblin et al., 2018). We employed the UAS-GAL4 system to
245 express transgenes (Brand et al., 1994) using the da-GAL4 driver line (Wodarz et al., 1995).
246 Embryo staging was achieved according to the Atlas of *Drosophila* Development (Hartenstein,
247 1993). Embryo sex was not determined, so both males and females were used indiscriminately.
248 Plasmids and fly lines can be obtained by contacting the corresponding author.

249

250 **Cell culture and transfection**

251 S2 cells, which were obtained from ATCC and used as is, were grown at room temperature in
252 Schneider's medium (Wisent Inc.) complemented with 10% fetal bovine serum (heat inactivated;

253 Wisent Inc.), 50 units/ml penicillin, and 50 □g/ml streptomycin (Life Technologies). S2 cells were
254 transfected at 60% confluency with FuGENE® (Promega) with selected pUASTattB-based
255 constructs together with pAct5c-GAL4. When indicated (24 h post-transfection), S2 cells were
256 treated with 10 □M ionomycin for 15 min, or 10 □M PAO and/or 1 □M□wortmannin for 45 min.

257

258 **Immunofluorescence**

259 In preparation for immunofluorescence on *D. melanogaster* embryos, the chorion was removed by
260 a 5 min incubation in a solution of 3% sodium hypochlorite. Embryos were then washed with water,
261 fixed for 8 min in 11% formaldehyde (diluted in 60 mM PIPES, 30 mM EGTA, 1.2 mM $MgSO_4$)
262 under a heptane phase (1:1), and rinsed with PBS. Embryos were devitellinized by vigorous
263 agitation in methanol. Non-specific binding sites were blocked by a 1 h incubation in NGT (2%
264 normal goat serum, 0.3% Triton X-100 in PBS). S2 cells were fixed 24 h post-transfection with
265 4% paraformaldehyde (in PBS) for 15 min, permeabilized with PBS-0,1% Triton X-100, and
266 saturated for 1 h with a solution of 2% normal goat serum and 0.1% Triton X-100 in PBS.

267 The following primary antibodies were used overnight at 4°C: anti-FLAG (M2, Sigma), 1:250 ;
268 anti-Yrt (Biehler et al., 2020), 1:500 ; anti-Lgl (d-300, Santa Cruz Technology), 1:100. Following
269 incubation with primary antibodies, embryos and cells were washed three times for 20 min in PBS
270 containing 0.3% or 0.1% Triton X-100 (PBT), respectively, and incubated for 1 h at room
271 temperature with Cy3- or Alexa Fluor 488-conjugated secondary antibodies (1:400). Unbound
272 secondary antibodies were washed-out with PBT (3 times 20 min). Embryos and cells were
273 mounted in Vectashield mounting medium (Vector Labs) and imaged by confocal microscopy.
274 Nuclei were stained with 4',6-diamidino-2-phénylindole (DAPI).

275

276 **Western blotting**

277 Dechorionated embryos were homogenized in lysis buffer (50 mM Tris-HCl pH 7.4, 150 mM
278 NaCl, 1 mM EDTA, 1% Triton X-100, 0.1 mM sodium orthovanadate, 0.1 mM
279 phenylmethylsulfonyl fluoride, 1 mM NaF, 10 µg/ml aprotinin, 10 µg/ml leupeptin and 0.7 µg/ml
280 pepstatin) at 4ºC and processed for SDS-PAGE and western blotting as described (Laprise et al.,
281 2002). The following primary antibodies were used: anti-FLAG M2 (Sigma-Adrich) 1:4000; anti-
282 GFP (Roche) 1:3000; anti-HA (BioLegend); anti-Actin (Novus Biologicals), 1:5000. Secondary
283 antibodies were conjugated to HRP (GE Healthcare) and diluted 1:2000. TrueBlot ULTRA
284 (Rockland) secondary antibodies were used for immunoprecipitation experiments (1:1000).

285

286 **Protein purification and lipid binding assays**

287 GST and GST-FERM expression in BL21 (DE3) cells was induced by adding 0.1 mM IPTG to
288 bacterial cultures (O.D. of 0.6 at 600 nm) for 16 h at 16ºC. Proteins were then purified as previously
289 described (Maity et al., 2013). PIP Strips membranes (P-6001; Echelon Biosciences) were saturated
290 with 3% fatty acid free BSA (Sigma-Aldrich A8806) in PBS-Tween-20 0.1% for 1 h at room
291 temperature. Membranes were then incubated with 1 µg of GST, GST-FERM, GST-VR, or
292 PI(4,5)P2 Grip (GST-PLC-d1-PH; Echelon Biosciences) following Echelon Biosciences' protocol.
293 Protein-lipid interactions were revealed by western blot using an anti-GST antibody (Santa Cruz
294 Biotechnology).

295

296 **Analysis of Yrt sequence**

297 Wild type and mutated sequences of the Yrt FERM domain were analyzed with the BH-search
298 algorithm [https://helixweb.nih.gov/bhsearch/ (Brzeska et al., 2010)].

299

300 **Quantification of membrane and cytoplasmic fluorescence intensity**

301 Quantification of fluorescence signal intensity was performed with FIJI (Schindelin et al., 2012).
302 In fly embryos, the polygon selection tool was used to generate a box, which was used to measure
303 both membrane and cytoplasmic intensity in each cell and the mean membrane/cytoplasm ratio
304 was determined. Ratios were determined in a total of 15 individual cells for each construct (5 non-
305 adjacent cells/embryo; 3 different embryos randomly selected from different experiments). Sample
306 size was empirically determined.

307

308 The freehand selection tool was used to individually select the whole membrane or cytoplasm in
309 S2 cells. This method was chosen, as the signal intensity was often irregular along the membrane
310 in S2 cells in contrast to what was observed *in vivo*. Total signal intensity (Raw Integrated Density;
311 RID) and the area of each box were recorded, and the membrane/cytoplasm ratios were calculated
312 as follow:

313 $$\text{Ratio} = \frac{(\text{membrane RID} \ / \ \text{membrane area})}{(\text{cytoplasm RID} \ / \ \text{cytoplasm area})}$$

314 Fluorescence ratio was quantified in 39 to 62 individual cells for each construct (10 to 23 cells per
315 experiment from 3-4 different experiments). The targeted sample size for S2 cells experiments was
316 about 45 cells, as we devised it would show sample variability and be sufficient to meet the normal
317 distribution assumption (true for samples treated with PAO and/or Wort).

318

319 **Viability test**

320 One hundred newly laid embryos of each genotype were collected and placed on an apple plate at
321 25ºC for 72 h (this experiment was performed in triplicate). Larvae and dead embryos were then
322 scored, and the ratio of larvae on larvae plus dead embryos x 100 represents the hatching
323 percentage. This sample size has been regularly used in our lab and allowed us to detect mild
324 lethality phenotypes (Gamblin et al., 2018).

325

326 **Immunoprecipitations**

327 HA immunoprecipitations were performed as previously described (Gamblin et al., 2018). For
328 GFP-Trap, S2 cells were homogenized in lysis buffer at 4ºC (50 mM Tris-HCl pH 7.4, 150 mM
329 NaCl, 1 mM EDTA, 1% Triton X-100, 0.1 mM sodium orthovanadate, 0.1 mM
330 phenylmethylsulfonyl fluoride, 1 mM NaF, 10 µg/ml aprotinin, 10 ºC g/ml leupeptin and 0.7 µg/ml
331 pepstatin. Cell lysates were centrifuged (17,000 g, 10 min at 4ºC) to remove insoluble cell
332 fragments. S2 cells lysates containing 2 mg of total proteins were precleared for 1.5 h under
333 agitation at 4 ºC with 15 µl of sepharose CL-4B beads (Sigma-Adrich). Supernatants were then
334 incubated with 15 µl of GFP-Trap beads (ChromoTek) for 1.5 h at 4ºC under agitation. Beads were
335 recovered by centrifugation and washed 5 times with lysis buffer. Immunocomplexes were eluted
336 with Laemmli's buffer.

337

338 **Statistical analysis**

339 Statistical analyses were performed with Prism 8 (GraphPad Software). Membrane-to-cytoplasmic
340 ratio were presented as violin plots showing all individual measures as well as median and quartiles.
341 As the data from the different groups were either not from a normal distribution and/or the sample
342 size was relatively small, the differences between individual groups were analyzed using the non-

343 parametric Kruskal-Wallis test and post-hoc Dunn's multiple comparison test, all compared to
344 FLAG-Yrt FL or DMSO (control conditions). Adjusted *p*-values <0.05 were considered
345 statistically significant. In the case of ionomycin treatment in S2 cells, a non-parametric Mann-
346 Whitney test, two-tailed with α=0.05 was performed to assess differences between treatments (as
347 the data were not from a normal distribution). For viability test, hatching data were presented as
348 means ± SEM. Differences between individual groups were analyzed by using Fisher's exact test
349 (95% confidence intervals, two-tailed). The significance threshold was adjusted in regards of the
350 multiple comparisons with a Bonferroni correction (8 comparisons). *P*-values <0.00625 were
351 considered statistically significant.
352

353 ## Figure legends

354 **Fig 1. The FERM domain of Yrt is necessary and sufficient for cortical targeting**
355 **(A)** Schematic representation of the FLAG-tagged proteins used in this study. **(B)** Stage 11 wild-
356 type embryo stained for Yrt. The picture depicts a portion of the ventral ectoderm. Scale bar
357 represents 10 µm. **(C-L)** FLAG and Lgl co-immunostaining in stage 10-11 embryos expressing
358 indicated FLAG-tagged constructs. Lgl staining was used to localize the membrane when needed
359 (only shown in D). **(M)** Violin plot showing the quantification of the membrane-to-cytoplasmic
360 ratio of each construct expressed in embryonic ectoderm (bold dotted line = median ; dotted lines
361 = quartiles). Data represents 15 non-adjacent cells per condition (5 cells per embryo from 3
362 different biological replicates). Kruskal-Wallis test followed by Dunn's multiple comparison test
363 compare different groups to FLAG-Yrt FL. Non-significant (ns) > 0.05 ; ** $P = 0.0024$; **** $P \leq$
364 0.0001.
365

366 **Fig 2. The FERM domain of Yrt associates with negatively charged phospholipids**

367 (**A**) PIP strip membranes were incubated with GST or indicated GST fusion proteins. (**B-F**) S2
368 cells were transfected with FLAG-Yrt and treated with indicated compounds (E-G). Cells were
369 then stained for FLAG. Scale bar represents 5 m. (**H-I**) Violin plots showing the quantification
370 of the membrane-to-cytoplasmic ratio in FLAG-Yrt expressing S2 cells presented in B-G (bold
371 dotted line = median ; dotted lines = quartiles). (**H**) Mann-Whitney test, two-tailed with statistical
372 significance set at $P < 0.05$, compares the difference between cells treated with DMSO (n= 49 cells
373 from 3 different experiments) or ionomycin (n=60 cells from 3 different experiments). (**I**) Kruskal-
374 Wallis test followed by Dunn's multiple comparison test compares each treated group (PAO : n=42
375 cells ; wort : n=40 cells ; PAO+wort : n=48 cells ; all from 3 different experiments) to vehicle
376 (DMSO ; n=39 cells from 3 different experiments). Non-significant (ns) > 0.05 ; * P=0.0265 ; ****
377 $P \leq 0.0001$.

378

379 (**A**) The black line in the upper panel shows the BH score (Y axis) along the wild-type sequence of
380 the Yrt FERM domain (X axis). Stretches of amino acids above the threshold of 0.6 are considered
381 BH motifs, which are underlined in the lower panel. The latter also displays mutations introduced
382 in the BH1 (orange) and the BH2 (purple and blue) motifs. The BH score of the mutant sequences
383 is also shown in the upper panel according to the same color code. (**B-C**) Immunostainings
384 performed with anti-FLAG antibodies in stage 10-11 embryos expressing indicated FLAG-tagged
385 constructs. Scale bar represents 10 m. (**D**) Violin plot showing the quantification of the
386 membrane-to-cytoplasmic ratio for FLAG-Yrt FL, FLAG-Yrt$^{BH1K/R>D}$ and FLAG-Yrt$^{BH2K>D}$
387 expressed the embryonic ectoderm (bold dotted line = median ; dotted lines = quartiles). Data
388 represent 15 non-adjacent cells per condition (5 cells per embryo from 3 different biological

389 replicates). (**E-G**) Immunostainings performed with anti-FLAG antibodies in S2 cells expressing
390 indicated FLAG-tagged constructs. Scale bar represents 5 □m. (**J**) Violin plot showing the
391 quantification of the membrane-to-cytoplasmic ratio for FLAG-GFP (n=62 cells from 4 different
392 experiments), FLAG-Yrt FL (n=62 cells from 4 different experiments), FLAG-Yrt$^{BH1K/R>D}$ (n=47
393 cells from 3 different experiments), FLAG-Yrt$^{BH2K>D}$ (n=46 cells from 3 different experiments)
394 and FLAG-Yrt $^{BH2K>D,K>A}$ (n=47 cells from 3 different experiments) expressed in S2 cells (bold
395 dotted line = median ; dotted lines = quartiles). (**D, J**) Kruskal-Wallis test followed by Dunn's
396 multiple comparison test compare each group to FLAG-Yrt FL. * $P = 0.0200$; ** $P = 0.0042$; ****
397 $P \leq 0.0001$.
398
399 **Fig 4. Yrt association with the lateral membrane is functionally important**
400 (**A**) Histogram showing the hatching rate, calculated in percentage, of embryos expressing
401 indicated FLAG-tagged Yrt proteins. Data are shown as means ± SEM, and statistical significance
402 was assessed by using a two-tailed Fisher's exact test (FL: $n = 269$; FERM-FA: $n = 234$; ΔFERM:
403 $n = 270$; FA-VR: $n = 233$; VR: $n = 269$; VRΔPBM: $n = 235$; BH1K/R>D: $n = 237$; BH2K>D: $n =$
404 265; 5D: $n = 247$; all from 3 different experiments). The significance threshold was adjusted in
405 regards of the multiple comparisons with a Bonferroni correction (8 comparisons). Non-significant
406 (ns) > 0.00625 ; **** $P \leq 0.0001$. (**B**) Western blot showing the relative expression of indicated
407 FLAG-tagged constructs in stage 11-12 embryos. Actin was used as loading control. (**C**) S2 cells
408 were transfected with indicated FLAG- and HA-tagged constructs. Immunoprecipitations with
409 anti-HA antibodies were then performed. (**D**) S2 cells expressing GFP-tagged transmembrane and
410 cytoplasmic domain of Crb and indicated FLAG-tagged Yrt proteins were homogenized and
411 submitted to GFP-Trap immunoprecipitations.

Acknowledgments

We acknowledge Konrad Basler, Nicolas Bisson, Sébastien Carréno, Ulrich Tepass, and the Bloomington *Drosophila* Stock Center for reagents. Flybase was used as an important database for this work. This work was supported by operating grants from the Canadian Institute of Health Research (CIHR) to P.L. (PJT-185951) and M.L. (PJT-178198). F.C. is supported by a scholarship from FRQ-S, and C. B. is a postdoctoral Europe Horizon MSCA-PF grantee.

Author contributions

P.L. conceived the project. C.G., C.A., F.C., F.P.P. and N.M. performed experiments and/or prepared reagents and contributed to data analysis. C.B. trained C.A. and contributed to initial *in vivo* analyses. A.J. performed statistical analysis and assembled figures with C.G. and C.A. P.L. wrote the manuscript, which was proofread by co-authors. P.L. and M.L. secured funding.

Competing interests

The authors declare no competing interests.

427 **REFERENCES**

428 **Bailey, M. J. and Prehoda, K. E.** (2015). Establishment of Par-Polarized Cortical
429 Domains via Phosphoregulated Membrane Motifs. *Dev Cell* **35**, 199-210.

430 **Baines, A. J.** (2006). A FERM-adjacent (FA) region defines a subset of the 4.1
431 superfamily and is a potential regulator of FERM domain function. *BMC Genomics* **7**, 85.

432 **Banerjee, S., Sousa, A. D. and Bhat, M. A.** (2006). Organization and function of septate
433 junctions: an evolutionary perspective. *Cell Biochem Biophys* **46**, 65-77.

434 **Barnett, K. C., Coronas-Serna, J. M., Zhou, W., Ernandes, M. J., Cao, A.,**
435 **Kranzusch, P. J. and Kagan, J. C.** (2019). Phosphoinositide Interactions Position cGAS at the
436 Plasma Membrane to Ensure Efficient Distinction between Self- and Viral DNA. *Cell* **176**, 1432-
437 1446 e11.

438 **Bieber, A. J., Snow, P. M., Hortsch, M., Patel, N. H., Jacobs, J. R., Traquina, Z. R.,**
439 **Schilling, J. and Goodman, C. S.** (1989). Drosophila neuroglian: a member of the
440 immunoglobulin superfamily with extensive homology to the vertebrate neural adhesion
441 molecule L1. *Cell* **59**, 447-60.

442 **Biehler, C., Rothenberg, K. E., Jette, A., Gaude, H. M., Fernandez-Gonzalez, R. and**
443 **Laprise, P.** (2021). Pak1 and PP2A antagonize aPKC function to support cortical tension
444 induced by the Crumbs-Yurt complex. *Elife* **10**.

445 **Biehler, C., Wang, L. T., Sevigny, M., Jette, A., Gamblin, C. L., Catterall, R.,**
446 **Houssin, E., McCaffrey, L. and Laprise, P.** (2020). Girdin is a component of the lateral polarity
447 protein network restricting cell dissemination. *PLoS Genet* **16**, e1008674.

448 **Brand, A. H., Manoukian, A. S. and Perrimon, N.** (1994). Ectopic expression in
449 Drosophila. *Methods Cell Biol* **44**, 635-54.

450 **Brzeska, H., Guag, J., Remmert, K., Chacko, S. and Korn, E. D.** (2010). An
451 experimentally based computer search identifies unstructured membrane-binding sites in
452 proteins: application to class I myosins, PAKS, and CARMIL. *J Biol Chem* **285**, 5738-47.

453 **Buckley, C. E. and St Johnston, D.** (2022). Apical-basal polarity and the control of
454 epithelial form and function. *Nat Rev Mol Cell Biol*.

455 **Dong, W., Zhang, X., Liu, W., Chen, Y. J., Huang, J., Austin, E., Celotto, A. M.,**
456 **Jiang, W. Z., Palladino, M. J., Jiang, Y. et al.** (2015). A conserved polybasic domain mediates
457 plasma membrane targeting of Lgl and its regulation by hypoxia. *J Cell Biol* **211**, 273-86.

458 **Ehret, T., Heissenberg, T., de Buhr, S., Aponte-Santamaria, C., Steinem, C. and**
459 **Grater, F.** (2023). FERM domains recruit ample PI(4,5)P(2)s to form extensive protein-
460 membrane attachments. *Biophys J* **122**, 1325-1333.

461 **Gamblin, C. L., Hardy, E. J., Chartier, F. J., Bisson, N. and Laprise, P.** (2014). A
462 bidirectional antagonism between aPKC and Yurt regulates epithelial cell polarity. *J Cell Biol*
463 **204**, 487-95.

464 **Gamblin, C. L., Parent-Prevost, F., Jacquet, K., Biehler, C., Jette, A. and Laprise, P.**
465 (2018). Oligomerization of the FERM-FA protein Yurt controls epithelial cell polarity. *J Cell*
466 *Biol*.

467 **Gassama-Diagne, A., Yu, W., ter Beest, M., Martin-Belmonte, F., Kierbel, A., Engel,**
468 **J. and Mostov, K.** (2006). Phosphatidylinositol-3,4,5-trisphosphate regulates the formation of
469 the basolateral plasma membrane in epithelial cells. *Nat Cell Biol* **8**, 963-70.

470 **Groth, A. C., Fish, M., Nusse, R. and Calos, M. P.** (2004). Construction of transgenic
471 Drosophila by using the site-specific integrase from phage phiC31. *Genetics* **166**, 1775-82.

472 **Hartenstein, V.** (1993). Atlas of Drosophila development. Plainview, N.Y.: Cold Spring
473 Harbor Laboratory Press.

474 **Hoover, K. B. and Bryant, P. J.** (2002). Drosophila Yurt is a new protein-4.1-like
475 protein required for epithelial morphogenesis. *Dev Genes Evol* **212**, 230-8.

476 **Krahn, M. P.** (2020). Phospholipids of the Plasma Membrane - Regulators or
477 Consequence of Cell Polarity? *Front Cell Dev Biol* **8**, 277.

478 **Laprise, P., Beronja, S., Silva-Gagliardi, N. F., Pellikka, M., Jensen, A. M., McGlade,**
479 **C. J. and Tepass, U.** (2006). The FERM protein Yurt is a negative regulatory component of the
480 Crumbs complex that controls epithelial polarity and apical membrane size. *Dev Cell* **11**, 363-74.

481 **Laprise, P., Chailler, P., Houde, M., Beaulieu, J. F., Boucher, M. J. and Rivard, N.**
482 (2002). Phosphatidylinositol 3-kinase controls human intestinal epithelial cell differentiation by
483 promoting adherens junction assembly and p38 MAPK activation. *J Biol Chem* **277**, 8226-34.

484 **Laprise, P., Lau, K. M., Harris, K. P., Silva-Gagliardi, N. F., Paul, S. M., Beronja, S.,**
485 **Beitel, G. J., McGlade, C. J. and Tepass, U.** (2009). Yurt, Coracle, Neurexin IV and the
486 Na(+),K(+)-ATPase form a novel group of epithelial polarity proteins. *Nature* **459**, 1141-5.

487 **Laprise, P., Paul, S. M., Boulanger, J., Robbins, R. M., Beitel, G. J. and Tepass, U.**
488 (2010). Epithelial polarity proteins regulate Drosophila tracheal tube size in parallel to the
489 luminal matrix pathway. *Curr Biol* **20**, 55-61.

490 **Maity, R., Pauty, J., Krietsch, J., Buisson, R., Genois, M. M. and Masson, J. Y.**
491 (2013). GST-His purification: a two-step affinity purification protocol yielding full-length
492 purified proteins. *J Vis Exp*, e50320.

493 **Martin-Belmonte, F., Gassama, A., Datta, A., Yu, W., Rescher, U., Gerke, V. and**
494 **Mostov, K.** (2007). PTEN-mediated apical segregation of phosphoinositides controls epithelial
495 morphogenesis through Cdc42. *Cell* **128**, 383-97.

496 **Ohata, S., Aoki, R., Kinoshita, S., Yamaguchi, M., Tsuruoka-Kinoshita, S., Tanaka,**
497 **H., Wada, H., Watabe, S., Tsuboi, T., Masai, I. et al.** (2011). Dual roles of Notch in regulation
498 of apically restricted mitosis and apicobasal polarity of neuroepithelial cells. *Neuron* **69**, 215-30.

499 **Sparks, L. M., Moro, C., Ukropcova, B., Bajpeyi, S., Civitarese, A. E., Hulver, M.**
500 **W., Thoresen, G. H., Rustan, A. C. and Smith, S. R.** (2011). Remodeling lipid metabolism and
501 improving insulin responsiveness in human primary myotubes. *PLoS One* **6**, e21068.

502 **Tepass, U.** (2009). FERM proteins in animal morphogenesis. *Curr Opin Genet Dev* **19**,
503 357-67.

504 **Wodarz, A., Hinz, U., Engelbert, M. and Knust, E.** (1995). Expression of crumbs
505 confers apical character on plasma membrane domains of ectodermal epithelia of Drosophila.
506 *Cell* **82**, 67-76.

507 **Wymann, M. P., Zvelebil, M. and Laffargue, M.** (2003). Phosphoinositide 3-kinase
508 signalling--which way to target? *Trends Pharmacol Sci* **24**, 366-76.

509

510

511

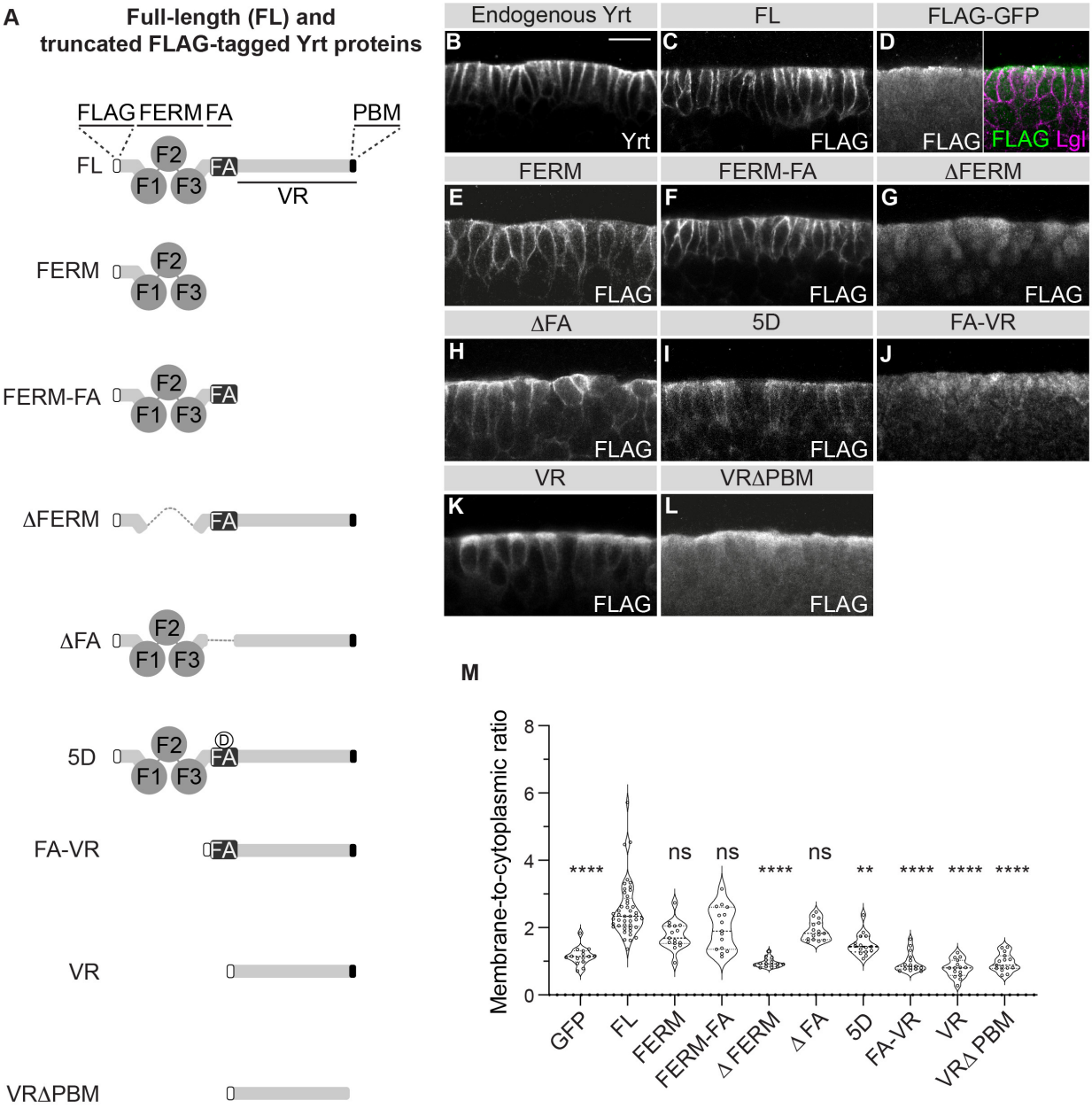

Gamblin et al. Fig. 1

512

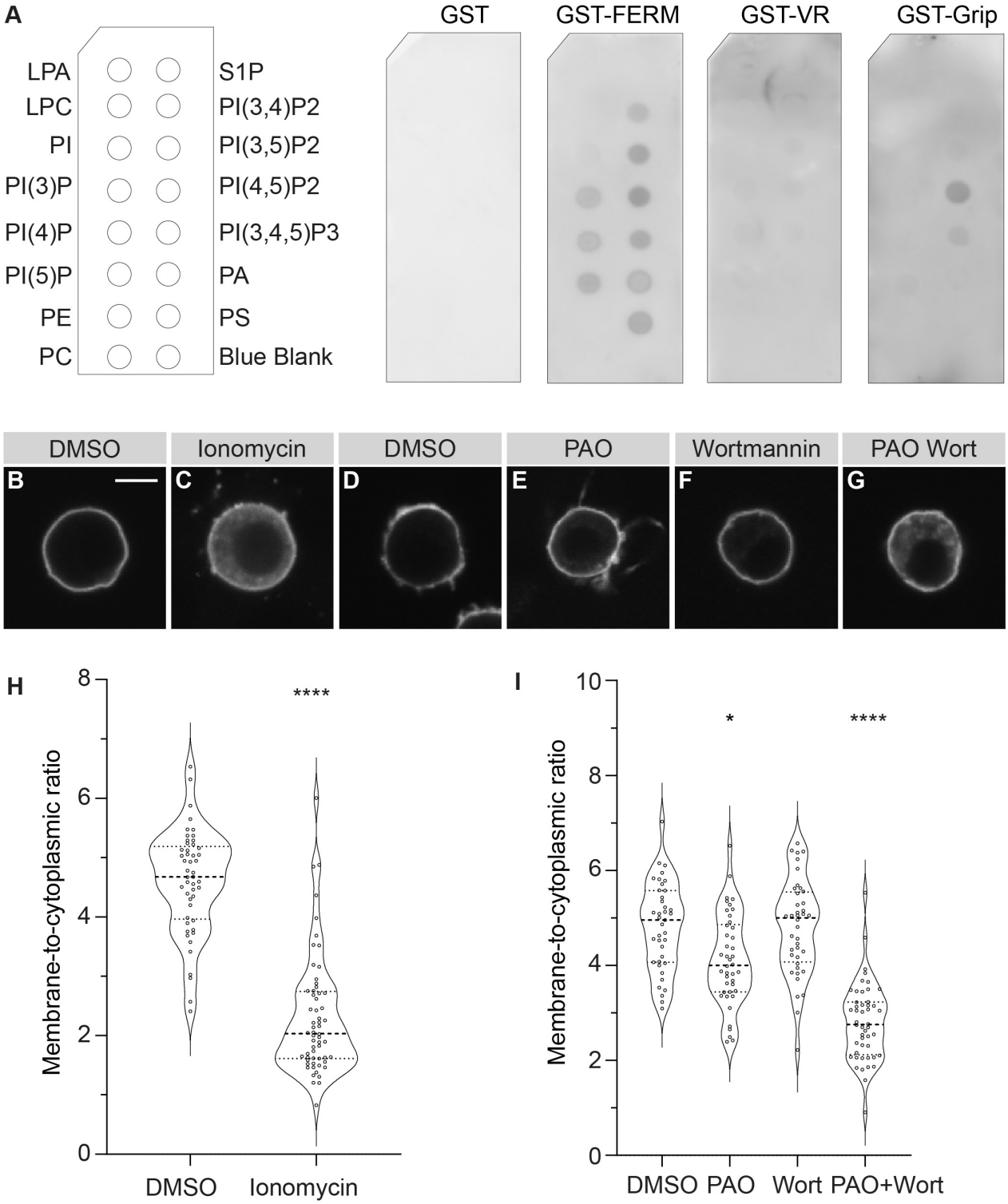

Gamblin et al. Fig. 2

513

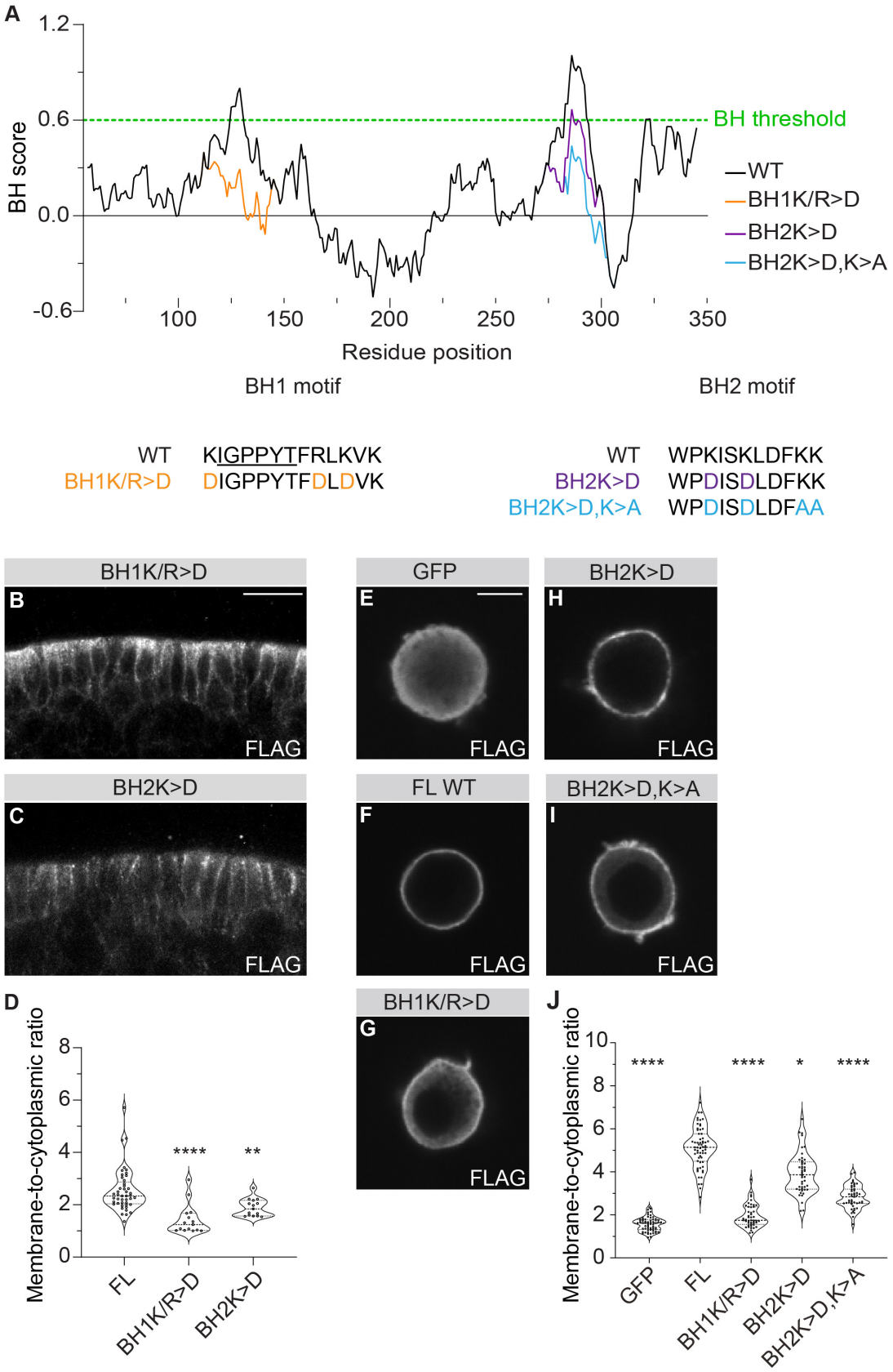

Gamblin et al. Fig. 3

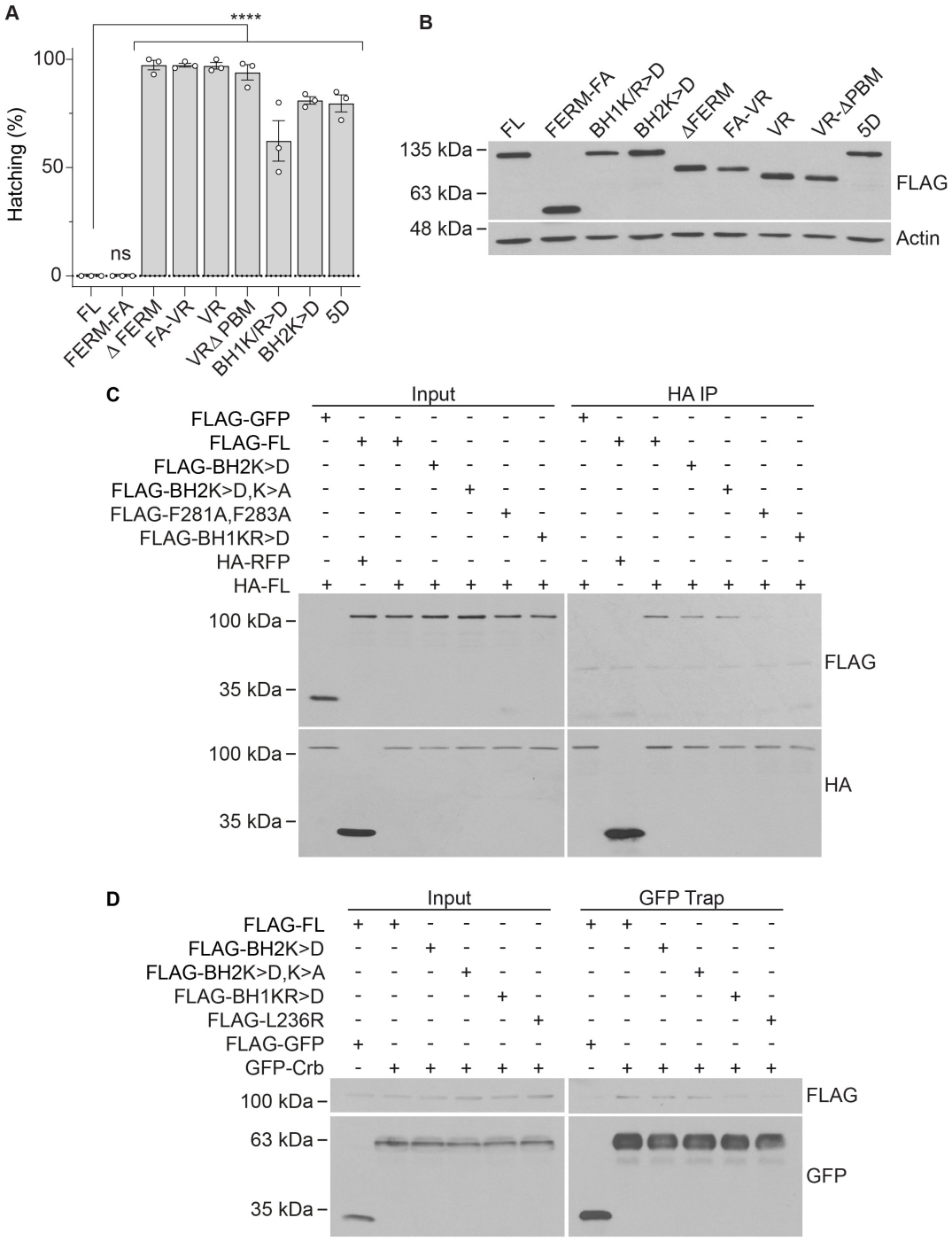

514

Gamblin et al. Fig. 4

BH1 motif

```
Yrt_drosophila        iekdyfglqfmdanhvkhwldptkpikkqvkigppytfrlkvkfyssepntlreeltryl 153
EPB41L5_human         iesdyfglrfmdsaqvahwldgtksikkqvkigspyclhlrvkfyssepnnlreeltryl 138
Epb41l5_mouse         iesdyfglrfmdsaqvahwldgtksikkqvkigspyclhlrvkfyssepnnlreeltryl 138
Epb41l5_rat           iesdyfglrfmdsaqvahwldgtksikkqvkigspyclhlrvkfyssepnnlreeltryl 138
epb41l5_zebrafish     vekdyfglrfmdsaqvphwldvtksikkqvkigppyclhmrvkfyssepnnlheeltryl 138
EPB41L4B_human        vetdyfglqfldsaqvahwldhakpikkqmkigpayalhfrvkyyssepnnlreeftryl 180
Epb41l4b_mouse        vetdyfglqfldsaqvthwldhakpikkqmkvgpayalhfrvkyyssepnnlreeftryl 180
                      :*.*****:*:*: :* **** :* ****:*:*  * ::::**:******.*:**:****
```

BH2 motif

```
Yrt_drosophila        rdqkiglffwpkiskldfkkkkltlivieddd-------egreqehtfvfrlynekackh 326
EPB41L5_human         gdtkiglffwpkitrldfkknkltlvvveddd-------qgkeqehtfvfrldhpkackh 311
Epb41l5_mouse         getkiglffwpkitrldfkknkltlvvveddd-------qgkeqehtfvfrldhpkackh 311
Epb41l5_rat           getkiglffwpkitrldfkknkltlvvveddd-------qgkeqehtfvfrldhpkackh 311
epb41l5_zebrafish     getkiglffwpkitrldfkkckltlvvveddeqvmqeteegkeqehtfvfrmdhpkackh 318
EPB41L4B_human        gankiglffwpkitkmdfkkskltlvvveddd-------qgreqehtfvfrldsartckh 353
Epb41l4b_mouse        gankiglffwpkitkmdfkkskltlvvveddd-------qgreqehtfvfrldsartckh 353
                         **********:::**** ****:*:***:       :*:*********:   ::***
```

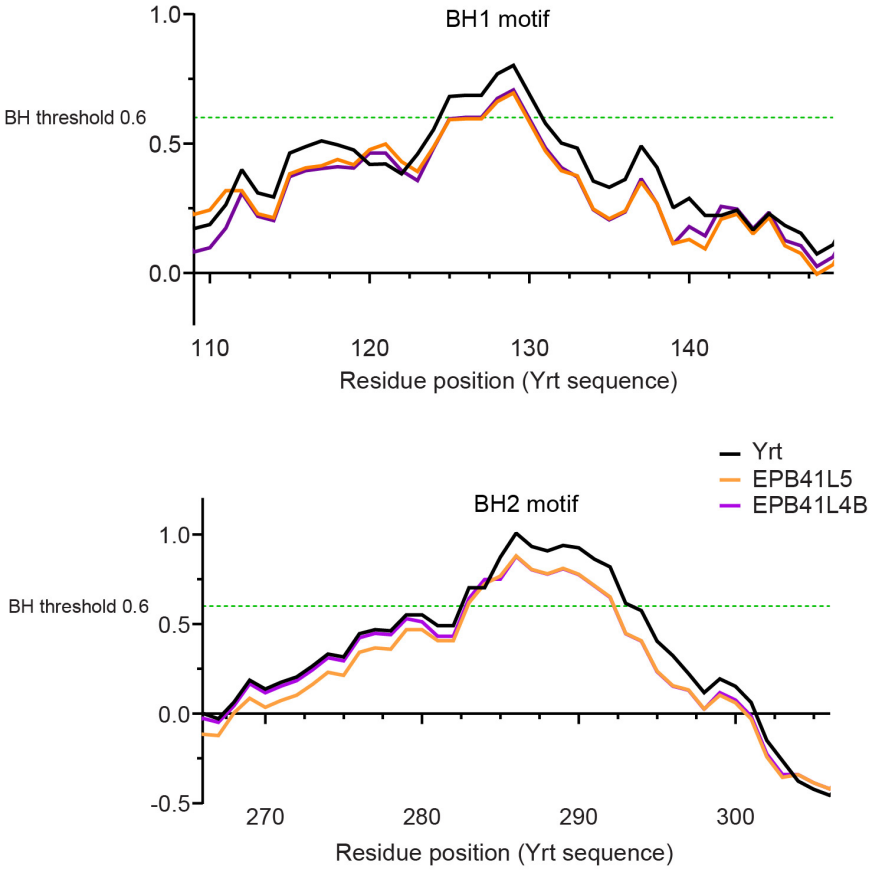

Figure S1. BH motifs in Yrt sequence are evolutionarily conserved. Alignment of the BH motifs of Yrt with the sequence of its two orthologs, namely EPB41L5 and EPB41L4B. Bottom panels show the BH score for Yrt sequence (black curve), or human EPB41L4B (purple curve) and EPB41L5 (orange curve) sequences. The BH1/2 scores of EPB41L4B and EPB41L5 go beyond the threshold of 0.6 even though their respective sequence diverges from Yrt sequence to some extent. Overall, these data suggest that Yrt orthologs also interact with the membrane using, among others, the conserved BH1 and BH2 motifs.